TRENDS IN SCIENCES 2025; 22(6): 9940 RESEARCH ARTICLE
https://doi.org/10.48048/tis.2025.9940

Integrated *In Vitro* and *In Silico* Exploration of Bioactive Compounds in *Strychnos lucida* Stem Extract: Revealing Mechanisms Against Breast Cancer

Yuslinda Annisa[1], Feri Eko Hermanto[2], Muhammad Hermawan Widyananda[1], Nuraini Rosyadah[1], Fairuz Sarah Kamila[1], Kavana Hafil Kusuma[1], Siti Mariyah Ulfa[3], Sri Rahayu Lestari[4], Fatchiyah Fatchiyah[1] and Nashi Widodo[1,*]

[1]*Department of Biology, Faculty Mathematics and Natural Science, Universitas Brawijaya, Malang 65145, Indonesia*
[2]*Division for Computational Biology, Faculty of Animal Science, Universitas Brawijaya, Malang 65145, Indonesia*
[3]*Department of Chemistry, Faculty Mathematics and Natural Science, Universitas Brawijaya, Malang 65145, Indonesia*
[4]*Department of Biology, Faculty Mathematics and Natural Science, Universitas Negeri Malang, Malang 65145, Indonesia*

([*]Corresponding author's e-mail: widodo@ub.ac.id)

Received: 6 February 2025, Revised: 24 February 2025, Accepted: 1 March 2025, Published: 10 May 2025

Abstract

Breast cancer remains the most commonly diagnosed cancer and the leading cause of cancer death in women worldwide. Numerous studies have explored various plant extracts as anticancer agents, targeting specific and effective cancer cell death pathways. This study aims to utilize *in vitro* and *in silico* approaches to evaluate the anti-breast cancer activity of *Strychnos lucida* and predict the molecular mechanisms of its active compounds. *In vitro* studies were performed by determining the total content of phenolics, flavonoids, terpenoids and alkaloids, examining toxicity and selectivity, apoptosis assay using Annexin V/PI and apoptosis morphology analysis using SEM, mitochondrial membrane potential (MMP) analysis using MitoTracker on T47D cells. *In silico* studies were used for compound analysis, anticancer compound candidate selection, target protein prediction, functional annotation, molecular docking and molecular dynamics simulation. The results of the *in vitro* study showed that phenolics were the class of compounds with the highest content in the *S. lucida* stem extract. The extract exhibited toxicity against T47D cells with an IC_{50} value of 734.79 µg/mL and general cytotoxicity against TIG-1 cells. The extract was able to induce apoptosis and changes in MMP in T47D cells. *In silico* study of *S. lucida* based on the KNApSAcK database contains 23 metabolites consisting of alkaloid, phenolic and glycoside groups. Six compounds are predicted to have anticancer activity, namely 3-O-caffeoylquinic acid, adenosine, loganine, secoxyloganin, sweroside and tachioside. These compounds target proteins associated with cancer development pathways, such as apoptotic pathways and the MAPK signaling pathway, and are predicted to inhibit cancer cell growth and induce apoptosis through their interaction with MAPK9 and MAPK3. *S. lucida* stem extract shows promising potential as an anticancer candidate; however, further *in vitro* studies are required to elucidate the specific mechanisms of action of its bioactive compounds in inhibiting breast cancer cells.

Keywords: *Strychnos lucida*, *In vitro*, *In silico*, T47D, Breast cancer, Apoptosis, MMP, MAPK9, MAPK3, 3-O-caffeoylquinic acid

Introduction

Breast cancer is the most widely diagnosed type of cancer and the most common cause of cancer-related death in women worldwide, with a prevalence of one-third of all types of cancer affecting women [1,2]. In numerous low-income and developing countries, including Indonesia, 50 - 80 % of breast cancer cases are

diagnosed at an advanced stage. At this point, the malignancy is often more challenging to manage, resulting in increased treatment costs and in many instances, leading to an incurable condition. [2]. Cancer treatment is commonly administered through surgical procedures, radiation therapy, and chemotherapy. However, these approaches can lead to considerable adverse effects, including elevated morbidity rates, the development of treatment resistance, and toxicity to normal cells. Consequently, there is a continuing search for effective alternative cancer therapies that provide lower morbidity, shorter recovery times, and non-invasive options [3,4].

In breast cancer, growth factors and chemokines activate multiple signaling cascades in a cross-talk manner involving receptor tyrosine kinases (RTKs) in the tumor microenvironment leading to cancer progression. RTKs are a group of single-pass transmembrane proteins that are expressed in various cell types including the tumor microenvironment. [5]. In addition, overexpression in breast cancer of various types of RTKs was found to be associated with increased aggressiveness of breast cancer [5,6]. Ligand binding causes conformational changes in RTKs that induce activation of important downstream signaling molecules, including mitogen-activated protein kinase (MAPK), Janus kinase/signal transducer and activator of transcription (JAK/STAT), and phosphoinositide 3-kinase (PI3K/Akt). RTK - regulated pathways play a key role in various aspects of cancer development, inducing cancer stem cell (CSC) phenotypes, as well as resistant responses to therapeutic regimens [5,7].

Currently, natural herbal medicines are gaining increased attention from researchers and the public due to their elucidated mechanisms of action, reduced side effects, and cost-effectiveness, leading to a growing interest in their potential application as therapies for cancer [8,9]. *Strychnos lucida*, locally referred to as *Doro Putih* or *Songa*, is a species within the Loganiaceae family that has long been utilized as a traditional medicinal resource in Bali and West Nusa Tenggara, Indonesia. *S. lucida* have a small tree; it can reach 30 cm in diameter and up to 12 m in height with a bitter taste of all parts of the plant. *S. lucida* is traditionally used by the local people to prevent and manage several diseases, including malaria, diabetes, inflammation, and cardiovascular problems. Phytochemical studies reported that *S. lucida* contains many active constituents such as beta-colubrine, brucine, brucine N-oxide, chlorogenic acid, diaboline, loganin, phyllamycin A, secoxyloganin, strychnine, strychnine N-oxide [10,11]. These compounds have demonstrated anticancer activity via various apoptotic mechanisms, including cell cycle inhibition, caspase pathway activation, and suppression of the MAPK signaling pathway [12-15].

Previous studies investigating the anticancer potential of bioactive compounds from *S. lucida*, particularly in relation to breast cancer, are still limited and insufficiently explored. Studies employing *in vitro* and *in silico* approaches to evaluate the potential of *S. lucida* as an anti-breast cancer agent are particularly effective for assessing the bioactivity of its compounds and elucidating the specific molecular mechanisms responsible for the cancer-inhibitory properties of its bioactive constituents. This study aims to assess the therapeutic efficacy of *S. lucida* stem extract against T47D breast cancer cell lines through of *in vitro* and *in silico* approaches.

Materials and methods

Extraction

The simplicia of *S. lucida* stem (Batch No. 220317.DRP.MLG.001) was obtained from the Herbal Materia Medica Laboratory, Batu, East Java, Indonesia. A total of 6 g of *S. lucida* simplicia and 60 mL of 96 % ethanol (1:10) were placed into a microwave-assisted extraction (MAE) vessel (Anton Paar, Austria). The MAE system was operated under the following conditions: The temperature was raised to 50 °C over 5 min, held at 50 °C for 15 min, and then cooled over 5 min, with a power setting of 1,500 W. After extraction, the filtrate was filtered using Whatman filter paper, and the solvent was evaporated using Rotary Evaporator Hei-VAP Expert (Heidolph, Korea) at 50 rpm and 50 °C. The resulting extract was obtained as a paste and stored at 4 °C.

Determination of total flavonoid content

The total flavonoid content was determined using the aluminum chloride ($AlCl_3$) colorimetric method and expressed as milligrams of quercetin equivalent per gram of extract (mg QE/g). A 50 µL aliquot of the *S. lucida* stem extract (1 mg/mL) or standard solution

(1.5625 - 400 µg/mL) was mixed with 150 µL of 96 % ethanol and 10 µL of 10 % $AlCl_3$. Subsequently, 10 µL of 1M sodium acetate (CH_3COONa) was added, and the mixture was incubated for 40 min at room temperature in the dark. Absorbance was measured at 405 nm using Multiskan SkyHigh Microplate Spectrophotometer (Thermo Fisher Scientific, USA), and the total flavonoid content was calculated based on the quercetin standard curve [16,17].

Determination of total phenolic content

The total phenolic content was determined using the Folin-Ciocalteu method and expressed as milligrams of gallic acid equivalent per gram of extract (mg GE/g). A 10 µL aliquot of the *S. lucida* stem extract (1 mg/mL) or standard solutions (1.5625 - 400 µg/mL) was mixed with 100 µL of Folin-Ciocalteu reagent (1:10, v/v). Subsequently, 1 µL of 7.5 % sodium carbonate (Na_2CO_3) solution was added, and the mixture was incubated for 90 min at room temperature in the dark. Absorbance was measured at 725 nm using Multiskan SkyHigh Microplate Spectrophotometer (Thermo Fisher Scientific, USA), and the total phenolic content was calculated based on the gallic acid standard curve [16,17].

Determination of total terpenoid content

The total terpenoid content was determined using linalool as a standard (0 - 63.66 µg/mL), following a modified method from Łukowski *et al.* [18]. A 1 mL of *S. lucida* stem extract (3 mg/mL) or linalool standard solution in methanol was added to a test tube along with 3 mL of chloroform, followed by homogenization using a vortex mixer. Subsequently, 500 µL of concentrated sulfuric acid (H_2SO_4) was slowly added, and the mixture was incubated at room temperature for 4 h in the dark. After incubation, a reddish-brown precipitate formed, which was retained. Then, 500 µL of 96 % methanol was added to the precipitate, and the mixture was vortexed until homogeneous. A 150 µL aliquot of the mixture was transferred to a 96-well plate, and absorbance was measured at 538 nm using Multiskan SkyHigh Microplate Spectrophotometer (Thermo Fisher Scientific, USA). The total terpenoid content was expressed as milligrams of linalool equivalent per gram of extract (mg LE/g) based on the regression equation from the linalool standard curve.

Determination of total alkaloid content

The total alkaloid content of *S. lucida* stem extract was determined using bromocresol green (BCG), following a modified method of Tan (2018). BCG (69.8 g) was dissolved in 3 mL of 2N NaOH and 5 mL of distilled water, and the solution was heated until fully dissolved. The extract (2 mg/mL) was dissolved in 2N HCl, filtered, and the pH was adjusted to neutral using 0.1N NaOH. A 1 mL aliquot of the extract solution and standard atropine solution (0 - 16,670 µg/mL) was added to 5 mL of BCG solution and 5 mL of phosphate buffer, and the mixture was homogenized. An equal volume of chloroform was then added, followed by vigorous shaking until a yellow complex formed at the bottom of the solution. The absorbance of both the standard and sample was measured at 470 nm using Multiskan SkyHigh Microplate Spectrophotometer (Thermo Fisher Scientific, USA). The total alkaloid content was expressed as milligrams of atropine equivalent per gram of extract (mg AE/g), calculated using the regression equation of the atropine standard curve [19].

Compound data mining

The active compounds present in the stems of *S. lucida* were sourced from the KNApSAcK database (http://www.knapsackfamily.com/KNApSAcK/), a comprehensive plant metabolite repository that includes data on 20,741 species and 50,048 metabolites [20]. The canonical SMILES representations for these compounds were retrieved from the PubChem database (https://pubchem.ncbi.nlm.nih.gov/).

Bioactivity and drug likeness screening

The prediction of cancer-related biological activities of the active compounds in *S. lucida* was conducted using the PASS Online web server (https://www.way2drug.com/passonline/) [21]. Pathway activities were selected based on their functions as anti-breast cancer agents, including anticancer activity, chemoprevention, treatment of proliferative diseases, JAK2 expression inhibition, TP53 expression enhancement, chemoprotection, apoptotic agonism, stimulation of caspase 3 and caspase 8, DNA synthesis inhibition, antimetastatic properties, antineoplastic effects, and inhibition of MMP9 expression. Compounds predicted to exhibit anticancer activity were further evaluated for drug-likeness using

the SWISS ADME web server (https://www.swissadme.ch/), which assesses medicinal properties based on the Lipinski, Ghose, Veber, Egan, and Muegge rules [17].

Proteins target prediction

Compounds from *S. lucida* that demonstrated potential anticancer activity and met drug-likeness criteria were further subjected to target protein prediction. Protein targets were identified using The Comparative Toxicogenomics Database (CTD) [22]. Predicted target proteins were subsequently analyzed for both direct and indirect protein-protein interactions using STRING 12.0 (https://string-db.org/). Visualization and sub-network analyses of these interactions were performed using Cytoscape 3.8.2. Proteins were ranked based on betweenness centrality, a metric used to evaluate a protein's significance in mediating interactions within the network, which facilitated the identification of critical target proteins [23].

Functional annotation

Functional annotation of the target proteins was conducted using the Database for Annotation, Visualization, and Integrated Discovery (DAVID) web server (https://david.ncifcrf.gov/). The analysis incorporated data from the Gene Ontology (GO) database, which classifies genes according to three domains - molecular function, biological process, and cellular component - and the Kyoto Encyclopedia of Genes and Genomes (KEGG) pathway database, which maps genes according to their involvement in cellular pathways [24].

Molecular docking

Molecular docking was conducted to confirm the binding interactions between the compounds and target proteins. The three-dimensional (3D) structures of the proteins were retrieved from the RCSB Protein Data Bank (https://www.rcsb.org/). Biovia Discovery Studio 2019 software (Dassault Systèmes, San Diego, CA, USA) was utilized to remove water molecules and contaminant ligands from the protein structures. The 3D structures of the selected compounds from *S. lucida* were obtained from the PubChem database (https://pubchem.ncbi.nlm.nih.gov/) and preprocessed using OpenBabel [25] integrated into PyRx 0.8 software. Specific docking was performed at the active sites of each protein using AutoDock Vina software [26] within PyRx 0.8. The resulting complexes from the docking analysis were visualized using Biovia Discovery Studio 2019 software.

Molecular dynamics simulation

Molecular dynamics simulations were conducted using YASARA (Yet Another Scientific Artificial Reality Application) software, employing the AMBER14 force field. The simulation parameters were set to mimic physiological cell conditions, including a temperature of 37 °C, pH 7.4, pressure of 1 atm, and a salt concentration of 0.9 %, and were run for 20 ns. Macro programs were utilized to evaluate the stability of the protein-ligand interactions: md_run for executing the simulation, md_analyze for root mean square deviation (RMSD) analysis, and md_bindingenergy for assessing the binding energy of the protein-ligand complex during the molecular dynamics process [17].

Cell culture preparation

T47D breast cancer cells and TIG-1 human fibroblast cells were obtained from the Laboratory of Animal Physiology, Structure, and Development at the Department of Biology, Faculty of Mathematics and Natural Sciences, Universitas Brawijaya. The T47D cells were cultured in RPMI 1,640 medium (Gibco, USA), while TIG-1 cells were cultured in MEM medium (Gibco, USA), both supplemented with 10 % fetal bovine serum (Gibco, USA) and 1 % penicillin-streptomycin (Gibco, USA). The cells were maintained at 37 °C with 5 % CO_2.

Cell viability assay

T47D and TIG-1 cells line were seeded at a density of 7,500 cells/well and incubated at 37 °C with 5% CO_2 for 24 h. Cells were subsequently treated with varying concentrations of *S. lucida* stem extract (0, 160, 320, 640 and 1,280 μg/mL) for 24 h. Following incubation, the treatment medium was replaced with fresh medium containing 5 % WST-1 reagent (Sigma-Aldrich, USA), and cells were further incubated for 30 min. Absorbance was measured at 450 nm using Multiskan SkyHigh Microplate Spectrophotometer (Thermo Fisher Scientific, USA). Cell viability percentages for T47D

and TIG-1 were calculated using Eq. (1). The IC_{50} value was determined by applying linear regression to the relationship between cell viability percentages and extract concentrations [16].

$$\text{Cell viability (\%)} = \frac{\text{Abs}_{\text{sample}} - \text{Abs}_{\text{blank}}}{\text{Abs}_{\text{control}} - \text{Abs}_{\text{blank}}} \times 100\% \quad (1)$$

To evaluate the cytotoxic selectivity of the extract against cancer cells, the selectivity index (SI) was calculated by dividing the average IC_{50} value of normal cells (TIG-1) by that of cancer cells (T47D) in each independent experiment, using Eq. (2). SI values greater than 3 indicate high selectivity of the extract [27,28].

$$\text{Selectivity index (SI)} = \frac{\text{IC}_{50} \text{ of normal cell}}{\text{IC}_{50} \text{ of cancer cell}} \quad (2)$$

Apoptosis assay

T47D cells were seeded at a density of 50,000 cells in 500 µL of culture medium per well in 24-well plates and incubated at 37 °C with 5 % CO_2 for 24 h. Cells were then treated with *S. lucida* stem extract at concentrations of ½IC_{50}, IC_{50}, and 2IC_{50} for 24 h. After treatment, cells were harvested using the trypsinization method, stained with FITC-Annexin V/propidium iodide (PI) (BioLegend, USA), and incubated for 20 min in the dark at 4 °C. The stained cell suspensions were analyzed using FACS-Calibur flow cytometry (BD FACS Calibur, USA) and data were analyzed using Cell Quest software (BF Bioscience, USA) [29].

Morphological analysis of apoptotic cells

Morphological analysis of T47D cell apoptosis was conducted using scanning electron microscopy (SEM) with a modified protocol adapted from Ali *et al.* [30]. A total of 25,000 cells were seeded into 24-well plates containing 500 µL of culture medium and cover slips pre-coated with carbon tapes, followed by incubation at 37 °C with 5 % CO_2 for 24 h. Cells were treated with *S. lucida* stem extract at its IC_{50} concentration for 24 h. After incubation, the treatment medium was removed, and the cells were washed three times with PBS. Cells were then fixed with 300 µL of 2 % glutaraldehyde for 20 min and washed again with PBS, followed by a series of graded ethanol dehydrations (30, 50, 70, 80, 90 %, and 2 cycles in absolute ethanol), with each step performed for 1 min. Post-dehydration, cells were air-dried in a fume hood for 15 - 20 min, sputter-coated with gold using the Quorum Q300TD, and examined under a field-emission scanning electron microscope (FEI Quanta FEG 650) at the Integrated Research Laboratory - Universitas Brawijaya (LRT-UB).

Potential membrane mitochondria analysis

Mitochondrial membrane potential (MMP) analysis in T47D cells was conducted using a modified protocol based on the method of Pendergrass *et al.* [31]. Cover slips were first placed in each well of 24-well plates, after which 25,000 cells were seeded into 500 µL of culture medium per well and incubated at 37 °C with 5 % CO_2 for 24 h. The cells were then treated with *S. lucida* stem extract at concentrations of ½IC_{50}, IC_{50}, and 2IC_{50} for 24 h. Post-incubation, the cells were washed three times with PBS. Subsequently, 200 nM MitoTracker™ Red CMXRos (Thermo Fisher Scientific, USA) and 100 nM MitoTracker™ Green FM (Thermo Fisher Scientific, USA), prepared in serum-free culture medium, were added to each well. The cells were incubated for 30 min in the dark, followed by three additional PBS washes. The cells on the cover slips were then visualized using a Confocal Laser Scanning Microscope (CLSM) (OLYMPUS FV-1000, Japan) and analyzed with FluoView version 17a software (OLYMPUS, Japan).

Statistical analysis

All data were presented as mean ± standard deviation (SD), with each value representing the average of three independent experiments. Statistical analysis of the apoptosis and mitochondrial membrane potential (MMP) assay results was conducted using one-way analysis of variance (ANOVA), followed by Duncan's Multiple Range Test (DMRT) for post-hoc comparisons. Statistical significance was set at a probability level of $p < 0.05$.

Results and discussion

Total bioactive compounds: Flavonoids, phenolics, terpenoids, and alkaloids in *S. lucida* stem extract

Pharmacological analysis of herbal effects as anticancer agents can be evaluated *in vitro* and integrated with bioinformatics approaches to elucidate

specific molecular mechanisms of potential bioactive compounds in the inhibition of cancer-related signaling pathways [9]. The study focused on analyzing the pharmacological effects of *S. lucida* stem extracts in relation to the bioactivity of its compounds in breast cancer inhibition using an *in vitro* approach integrated with an *in silico* approach to determine the prediction of anticancer related activities. The ethanol extract of *S. lucida* stem was found to have the highest phenolic content, followed by flavonoids, alkaloids and terpenoids (**Table 1**). Phenolic compounds were found to be the most abundant, with a concentration of 202.917 ± 3.20 mg GAE/g. This indicates that phenols are the dominant class of bioactive compounds in the extract. Meanwhile, based on the KNApSAck database, the compounds in *S. lucida* stem are dominated by alkaloid and glycoside compounds, and there are several phenolic compounds (**Table 2**). Several studies have shown that the content of bioactive compounds of *S. lucida*, including triterpenoids, phenolics, alkaloids and flavonoids, are the main classes of compounds detected in this species, where different parts of the plant and the place of growth may affect the composition of chemical components [32].

Tabel 1 Total bioactive content (Flavonoids, Phenolics, Terpenoids, and Alkaloids) in *S. lucida* stem extract.

Bioactive content	***S. lucida* stem extract**
Total flavonoid content (TFC)	34.056 ± 3.14 mgQE/g
Total phenolic content (TPC)	202.917 ± 3.20 mgGAE/g
Total terpenoid content (TTC)	3.316 ± 1.05 mgLE/g
Total alkaloid content (TAC)	3.646 ± 0.92 mgAE/g

Note: Data are presented as mean ± SD, with each value representing the average of 3 independent experiments

Bioactive compounds based on database, probable activity and drug-likeness of compounds in *S. lucida* stems

Based on the KNApSAcK database, there are 23 bioactive compounds in *S. lucida* stems, dominated by alkaloid and glycoside compounds, as detailed in **Table 2** and **Figure 1**. Alkaloid compounds found in *S. lucida* are 11-methoxydiaboline; alpha-colubrine; beta-colubrine; brucine; brucine N-oxide; diaboline; loganate; pseudobrucine; pseudostrychnine; and strychnine. The alkaloid glycosides are loganine; normacusine B; and picconioside I. The phenolic glycosides are ligustrinoside; secoxyloganin; staunoside C; and sweroside. Saponin glycosides are sylvestroside I; tachioside; and triplostoside A. Two compounds containing triterpenoid glycosides are acanthoside B and cantleyoside. There are two phenolic compounds, namely 3-4-di-O-caffeoylquinic acid and 3-O-caffeoylquinic acid, and one nucleoside compound, namely adenosine.

Table 2 Bioactive compounds in *S. lucida* stem from the KNApSAcK database.

No	**Compound**	**Formula**	**MW (g/mol)**	**PubChem ID**
1	11-Methoxydiaboline	$C_{22}H_{26}N_2O_4$	382.189	13994712
2	3,4-di-O-caffeoylquinic acid	$C_{25}H_{24}O_{12}$	516.127	5281780
3	3-O-Caffeoylquinic acid	$C_{16}H_{18}O_9$	354.095	1794427
4	Acanthoside B	$C_{28}H_{36}O_{13}$	580.216	443024
5	Adenosine	$C_{10}H_{13}N_5O_4$	267.097	60961
6	alpha-Colubrine	$C_{22}H_{24}N_2O_3$	364.179	12303796

No	Compound	Formula	MW (g/mol)	PubChem ID
7	beta-Colubrine	$C_{22}H_{24}N_2O_3$	364.179	251890
8	Brucine	$C_{23}H_{26}N_2O_4$	394.189	442021
9	Brucine N-oxide	$C_{23}H_{26}N_2O_5$	410.184	273111
10	Cantleyoside	$C_{33}H_{46}O_{19}$	746.263	12302406
11	Diaboline	$C_{21}H_{24}N_2O_3$	352.179	12312946
12	Loganate	$C_{16}H_{24}O_{10}$	376.137	5460138
13	Loganin	$C_{17}H_{26}O_{10}$	390.153	87691
14	Normacusine B	$C_{19}H_{22}N_2O$	294.173	10469722
15	Picconioside I	$C_{33}H_{48}O_{18}$	732.284	274413064
16	Pseudobrucine	$C_{23}H_{26}N_2O_5$	410.184	3083630
17	Pseudostrychnine	$C_{21}H_{22}N_2O_3$	350.163	21723446
18	Secoxyloganin	$C_{17}H_{24}O_{11}$	404.132	162868
19	Strychnine	$C_{21}H_{22}N_2O_2$	334.168	441071
20	Sweroside	$C_{16}H_{22}O_9$	358.126	161036
21	Sylvestroside I	$C_{33}H_{48}O_{19}$	748.279	101967019
22	Tachioside	$C_{13}H_{18}O_8$	302.100	11962143
23	Triplostoside A	$C_{35}H_{52}O_{20}$	792.305	85118299

The selection of compounds in *S. lucida* stems was based on bioactivity assessment to predict the probable activity of compounds in inhibiting cancer progression using PASS Online. The screening process focused on compounds with a probability of activity (Pa) value equal to or greater than 0.3 [21]. Out of 23, 11 compounds met the criteria, namely 3-4-di-O-caffeoylquinic acid, 3-O-caffeoylquinic acid, acidacanthoside B, adenosine, cantleyoside, loganine, picconioside I, secoxyloganin, sweroside, sylvestroside I and tachioside (**Figure 1(A)**). The eleven compounds were then subjected to a drug likeness screening aimed at selecting compounds with drug-like properties with a violation value of not more than 2 (**Figure 1(B)**). Out of the 11, 6 compounds met the characteristics of drug compounds, namely 3-O-caffeoylquinic acid, adenosine, loganine, secoxyloganin, sweroside and tachioside (**Figure 1(C)**). The selected compounds were further evaluated by molecular docking analysis.

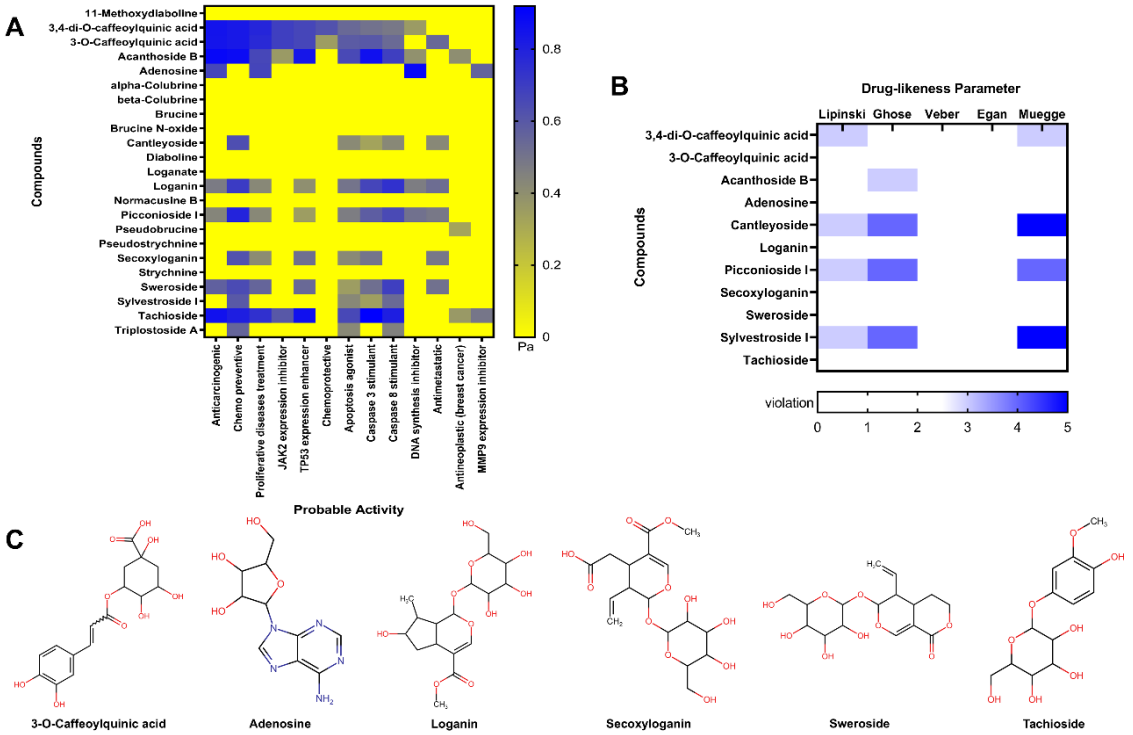

Figure 1 Profile of Bioactive Compounds in *S. lucida* Stem. (A) Bioactivity of compounds based on PASS Online analysis. (B) Drug-likeness screening of compounds based on Lipinski, Ghose, Veber, Egan and Muegge rules. (C) Six selected compounds meeting the parameters of probable activity and drug-likeness.

Protein target prediction of bioactive compounds in *S. lucida* stems and functional annotation related to cancer cell development

The protein target prediction yielded a total of 21 candidates, which were then analyzed using the betweenness centrality method. Betweenness centrality is derived from the proportion of shortest paths between 2 nodes that pass through the node under examination. In the context of protein-protein interaction (PPI) networks, target proteins with critical functional roles typically exhibit higher betweenness centrality values compared to others. This metric reflects the extent to which a protein serves as a bridge within the network. The betweenness value is determined based on the constructed multilayer network, representing the probability of a protein layer node being traversed during the network's dynamic processes [33,34]. The results from the proteins interaction identification analysis showed that 14 target proteins exceeded the score, starting from the top: TP53, CASP8, IL-6, CDKN1B, MAPK9, MAPK3, RELA, BCL-2, CASP3, FOS, MAPK8, MAPK1, JUN, and CCND1 (**Figure 2(A)**). Among these proteins, proteins that play a role in the MAPK pathway are potentially inhibited in the cancer progression pathway. Mitogen-activated protein kinases (MAPKs) are key regulators of cellular signaling, playing critical roles in many cellular processes including cell division/survival, differentiation, migration, transformation, gene expression, apoptosis and stress response [35,36]. Hyperactivation of the RAS/RAF/MAPK signaling pathway plays a critical role in cancer progression, and the development of targeted therapies against this pathway has demonstrated varying degrees of effectiveness across different cancer types [36]. Therefore, MAPK9, MAPK3, and MAPK8 were selected as the 3 primary target proteins based on their ranking according to betweenness centrality values.

.

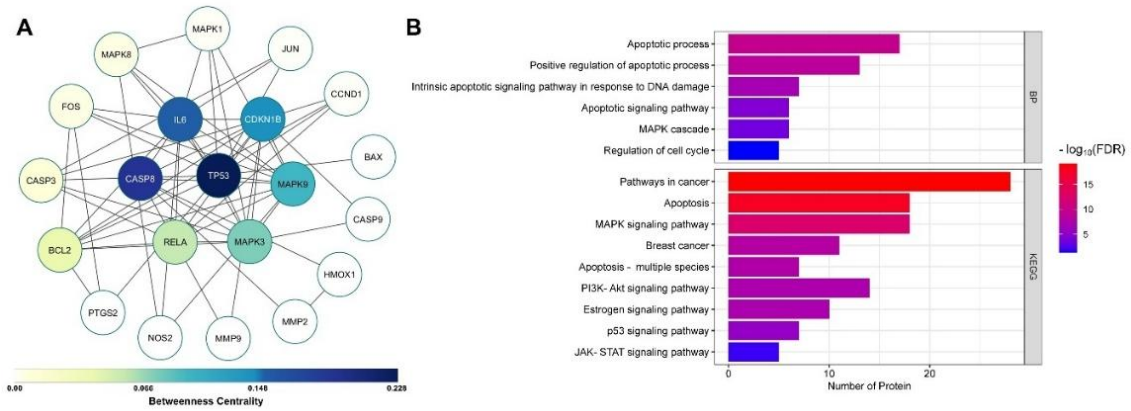

Figure 2 Determination of Target Proteins of Selected *S. lucida* Compounds. (A) Protein-Protein Interaction (PPI) with ranked values based on betweenness centrality. (B) Functional annotations associated with Biological Process (BP) and KEGG pathways associated with target proteins.

All target proteins have a role in cancer cell development based on GO analysis and KEGG pathway (**Figure 2(B)**). The biological process (BP)-related GO analysis showed the involvement of the target proteins in apoptotic process, positive regulation of apoptotic process, intrinsic apoptotic pathway in response to DNA damage, apoptotic pathway, MAPK cascade and cell cycle regulation. According to the KEGG pathway, the target protein plays a role in various cancer-related signaling pathways such as apoptosis, MAPK signaling pathway, breast cancer signaling pathway, PI3K-Akt, estrogen, p53, and JAK-STAT signaling pathway.

Molecular interaction among the bioactive compounds in *S. lucida* and the target proteins MAPK9, MAPK3, and MAPK8

Molecular docking simulations were performed on 6 bioactive compounds with 3 types of target proteins, as shown in **Table 3**. Docking results with the most negative binding affinity values between target proteins and bioactive compounds from *S. lucida* were found in MAPK9 and 3-O-caffeoylquinic acid (binding affinity −8.1 kcal/mol), MAPK3 with loganin, secoxyloganin, and sweroside (binding affinity −8.0 kcal/mol), and MAPK8 and 3-O-caffeoylquinic acid (binding affinity −7.4 kcal/mol). 3-O-Caffeoylquinic acid binds to MAPK9 by forming 4 hydrogen bonds and 2 hydrophobic bonds with the same residue as the control, Asp169. The results of docking with MAPK3 show that loganin has the most residues in common with the control, namely Met125, Lys131, Asp128, Asn171. Loganin binds to the active site of MAPK3 by forming 4 and 6 hydrophobic bonds. In addition, 3-O-caffeoylquinic acid binds to the active site of MAPK8 by forming 2 and 3 hydrophobic bonds with the same residue as the control, Ser155. The most negative binding affinity value from the docking results and the same number of amino acid residues as the control are the basis for selection for further molecular dynamics simulations (**Figure 3**).

Table 3 Molecular docking simulation result - The interaction between MAPK9, MAPK3, MAPK8, and Ligand.

Protein target	Ligand	Binding affinity (kcal/mol)	Hydrogen interaction	Hydrophobic interaction
MAPK9 PDB ID: 3npc	Control [37]	−7.6	Arg189, Thr188, **Asp169**	Val187, Asp151, Arg69, Arg72
	Loganin	−6.7	Gal37, Arg72, **Asp169**	Leu172, Tyr185
	3-O-Caffeoylquinic acid*	**−8.1**	Glu73, **Asp169**, Lys55, Met111	Val40, Met108
	Adenosine	−6.8	Gln37, Lys55, Arg69, Arg672, Asp151, **Asp169**, Gly171	

Protein target	Ligand	Binding affinity (kcal/mol)	Hydrogen interaction	Hydrophobic interaction
	Secoxyloganin	−6.7	Lys153, Tyr185, Gln37, Arg69, Arg72, Arg174, Leu172, Ala173, Asp151	
	Sweroside	−7.6	Thr183, Ala53, Lys55, Glu73, **Asp169**	Val158, Met111, Met108, Val40, Leu168, Phe170
	Tachioside	−7.6	Glu73, Ala53	Asp169, Phe170, Val40, Leu168
MAPK3 PBD ID: 2zoq	Control [38]	−8.3	**Lys131, Asp128**, Ser170, **Asn171**, Cys183, **Met125**	
	Loganin*	**−8.0**	**Met125, Lys131, Asp128, Asn171**	Val56, Cys183, Leu173, Ile48, Lys71, Gln122
	3-O-Caffeoylquinic acid	−7.5	**Lys131**, Glu50, Asp184	Leu173, Val56, Ala69, Lys183
	Adenosine	−7.9	Ser170, Asp184, Ile48, **Lys131, Asp128, Met125**	
	Secoxyloganin*	−8.0	Asp184, Asp128, **Lys131**	Cys183, Leu173, Ala69, Val56, Lys71, Asn171, Met125
	Sweroside*	−8.0	Ser170, **Asp128,** Asp184	Asn171, Lys131, Cys183, Leu173, Val56, Ala69
	Tachioside	−7.7	**Asp128**, Glu50, Gln122	Lys131, Cys183, Leu173, Ala69, Val56
MAPK8 PDB ID: 4g1w	Control [39]	−10.8	**Ser 155**	Ile32, Ile86, Val158, Val40, Ala53, Leu168, Met108
	Loganin	−7.1	**Ser155**, Asn114, Ala113	Ala53, Val40, Leu168, Val158, Ile32, Leu110
	3-O-Caffeoylquinic acid*	**−7.4**	Met111, **Ser155**	Val158, Leu168, Ala53
	Adenosine	−6	Arg69, Leu172, Gly171	
	Secoxyloganin	−6.4	Gly38, Lys55, Phe170, Gly171, Asp169	
	Sweroside	−7	Lys55, Leu168	Phe170
	Tachioside	−6.1	Lys55, Arg72	Glu73

*Bioactive compounds in *S. lucida* with the most negative binding affinity when interacting with target proteins compared to other compounds.

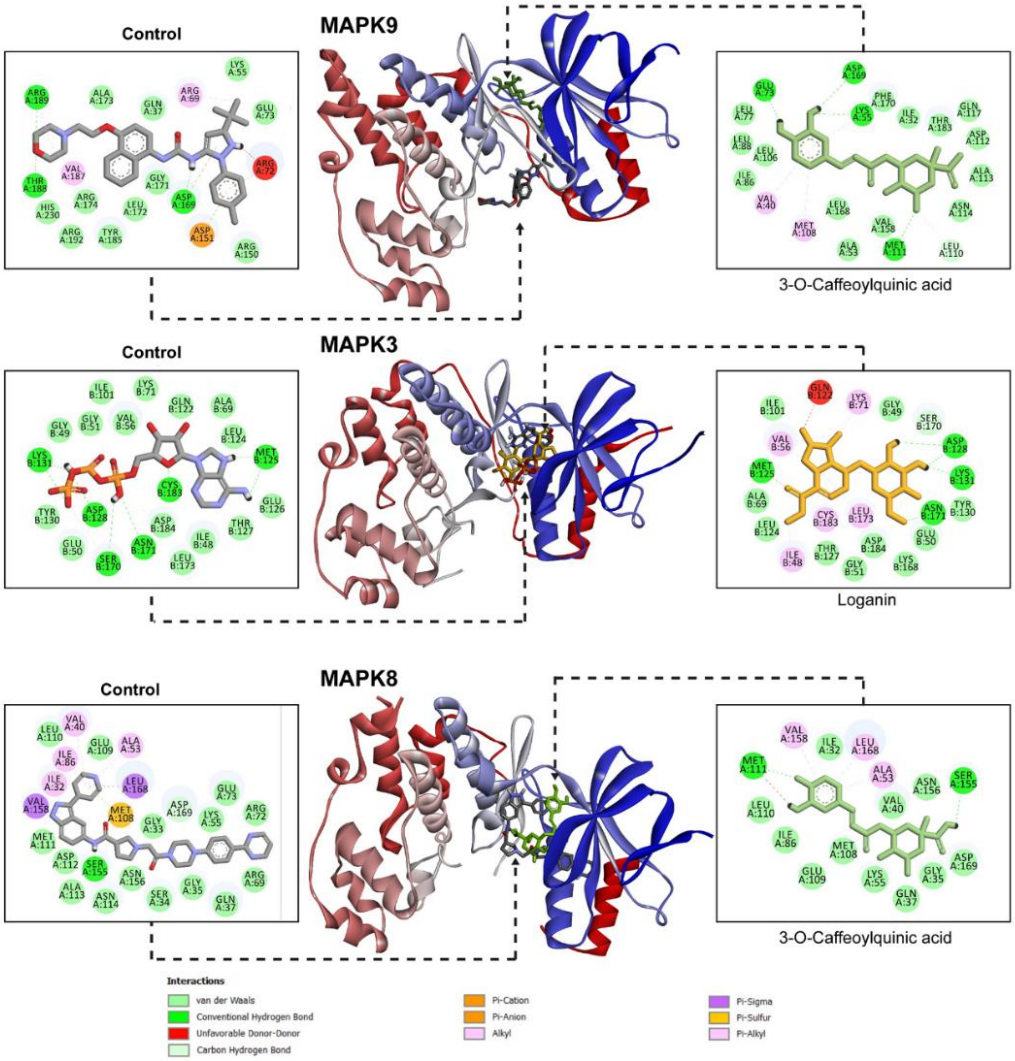

Figure 3 Molecular docking simulation results of target protein, control, and the selected *S. lucida* bioactive compound with the most negative binding affinity

Stability of interactions between bioactive compounds in *S. lucida* and the target proteins MAPK9, MAPK3, and MAPK8

Molecular dynamics analysis to determine conformational stability and binding between ligands and proteins in terms of structural stability, conformational flexibility and folding. Molecular dynamics simulations were performed for 20 ns to evaluate the RMSD value and binding energy between protein-ligand [40]. The results of the molecular dynamics analysis showed that the RMSD values of the protein-ligand complexes of the *S. lucida* compounds had relatively stable RMSD values, especially the MAPK9 complex and its ligand showed stable motion during the simulation. Loganin has a more stable RMSD value compared to the control, because the RMSD movement value of the control ligand after binding to MAPK3 increases from the beginning of the simulation to the end of the simulation. Meanwhile, the RMSD of the movement of the 3-O-caffeoylquinic acid ligand after binding to MAPK8 increases at ~7 ns, but stabilizes again from ~12 ns to the end of the simulation (**Figure 4(A)**). The average RMSD value of each *S. lucida* compound protein-ligand complex remained below 3 Å throughout the simulation process, indicating that the simulated system has good stability and does not deviate much from the initial structure [17,40].

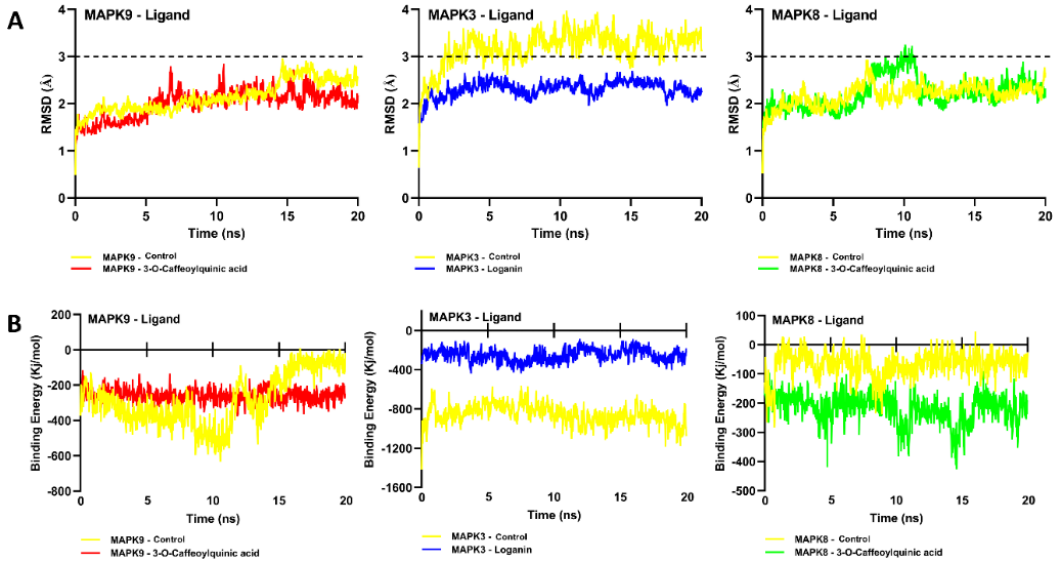

Figure 4 Molecular dynamics simulation results of target protein, control and the selected *S. lucida* bioactive compound. (A) Root mean square deviation (RMSD) of the protein-compound complex. (B) Molecular dynamics binding energy of each complex.

The results of the molecular dynamics binding energy analysis show that the MAPK9 - 3-O-caffeoylquinic acid and MAPK3 - loganin complex interactions have binding energy values that are more stable than the control and have more positive binding energy values than the control (**Figure 4(B)**). The MAPK8 - 3-O-caffeoylquinic acid complex has a binding energy value that is much more negative than the control. The binding energy value is used to determine the stability of the interaction between protein-ligand complexes; the more positive the binding energy value, the more stable the protein-ligand interaction [17]. Overall, molecular dynamics simulations show that the interaction between proteins and compounds present in *S. lucida* is more stable in the MAPK9-3-O-caffeoylquinic acid and MAPK3-loganin complexes, and that these compounds have the potential to act as inhibitors of related proteins.

Mitogen-activated protein kinase 3 (MAPK3) or extracellular signal-regulated kinase 1 (ERK1) is a cell signalling molecule of the ERK/MAPK pathway that plays a critical role in mediating the transduction of signals that regulate apoptosis, cell proliferation and cell migration through the activation of nuclear transcription factors such as c-Jun and c-Fos. MAPK3 overexpression and/or hyperactivity is known to be closely associated with cancer cell initiation, progression, migration and drug resistance in several cancers, including liver, thyroid, lung and gastric cancers [41]. Loganin is a class of alkaloid glycosides known to reduce the expression of BCL-2, which can induce cancer cell death, induce cell cycle arrest and suppress proliferation through the ERK1/2 pathway, block the PI3K/AKT/mTOR pathway, and suppress the expression of p-ERK and p-p38 proteins, resulting in inhibition of MAPK pathway activation [42]. Functional annotation of the KEGG pathway also shows that loganin target proteins are involved in several related pathways such as the MAPK, PI3K-AKT and JAK-STAT pathways, including the estrogen signalling pathway (**Figure 2(B)**). In breast cancer signaling pathways, activation of MAPK and PI3K/Akt pathways by EGFR and HER2 contributes to ERα phosphorylation, especially ERα phosphorylation at serine 118 which plays a role in endocrine therapy resistance. Therapies targeting inhibition of both EGFR and ERα pathways are more effective than single treatments targeting ERα to avoid therapy resistance [43].

Toxicity of *S. lucida* stem extract on T47D breast cancer cells

Cytotoxicity assays of *S. lucida* stem extract showed an increase in toxicity to T47D cells with increasing extract concentration, with an IC_{50} value of 734.79 ± 80.99 µg/mL (**Figure 5**). Previous research reported that ethyl acetate extract of *S. lucida* stem can

inhibit up to 70 % of the viability of the T lymphoblast cell line MOLT-3 [32]. Studies investigating *S. lucida* on cancer cells are still very limited. The potential to evaluate the bioactivity of compounds in this plant is still very high. The evaluation related to the selectivity of the extract on normal TIG-1 cells with an IC_{50} value of 980.45 ± 80.47 µg/mL showed an SI value of 1.33, which is classified as general cytotoxicity [44]. Maximum cytotoxicity against cancer cells and low damage to normal cells is a favorable consideration in the development of cancer therapy, demonstrating the selectivity of the anticancer mechanism [45]. Despite the lack of selectivity, the *S. lucida* stem extract still has a lower IC_{50} value on cancer cells. In addition, the severe reduction in TIG-1 cell viability only occurred above the concentration 640 µg/mL. This indicates that the potential toxicity of the extract on cancer cells is predominant rather than on normal cells. To further investigate its cytotoxic potential against breast cancer cells, the extract's effects on apoptosis and mitochondrial membrane potential (MMP) were subsequently assessed.

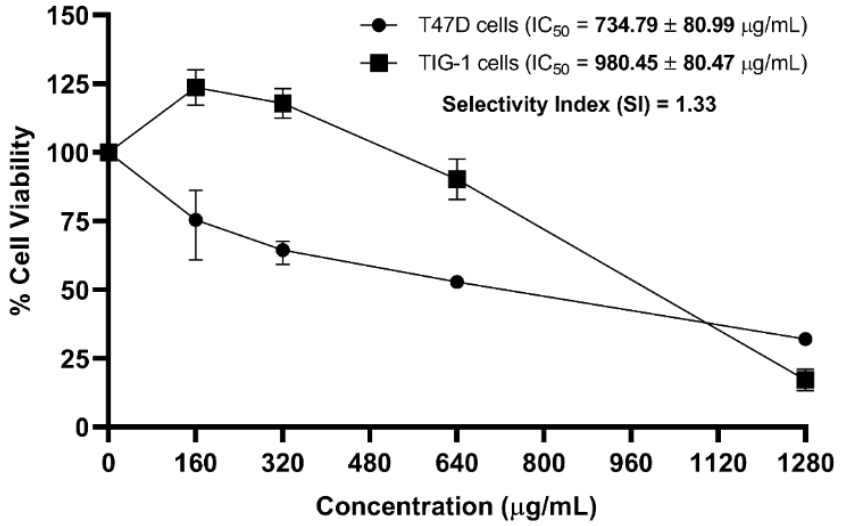

Figure 5 Cytotoxicity of *S. lucida* Stem Extract on T47D and TIG-1 Cell Lines and its Selectivity Index (SI). Data are expressed as mean ± SD, with each value representing the average of three independent experiments.

***S. lucida* stem extract induced apoptosis of T47D cells**

Apoptosis induction of *S. lucida* stem extract on T47D cells was evaluated using propidium iodide (PI) and annexin V to determine the relative number of live, apoptotic and necrotic cells. Meanwhile, the morphology of apoptosis in T47D cells was assessed using SEM. Annexin V is capable of binding to phosphatidyl serine, which translocated to the outer plasma membrane during apoptosis, whereas PI binds to DNA in necrotic cells [46,47]. *S. lucida* stem extract was able to induce apoptosis in T47D cells, which increased with increasing extract concentration (**Figure 6(A)**). The highest increase in apoptosis was 16.02 ± 3.54 % at an extract concentration of 1,469.58 µg/mL (**Figures 6(A) - 6(B)**).

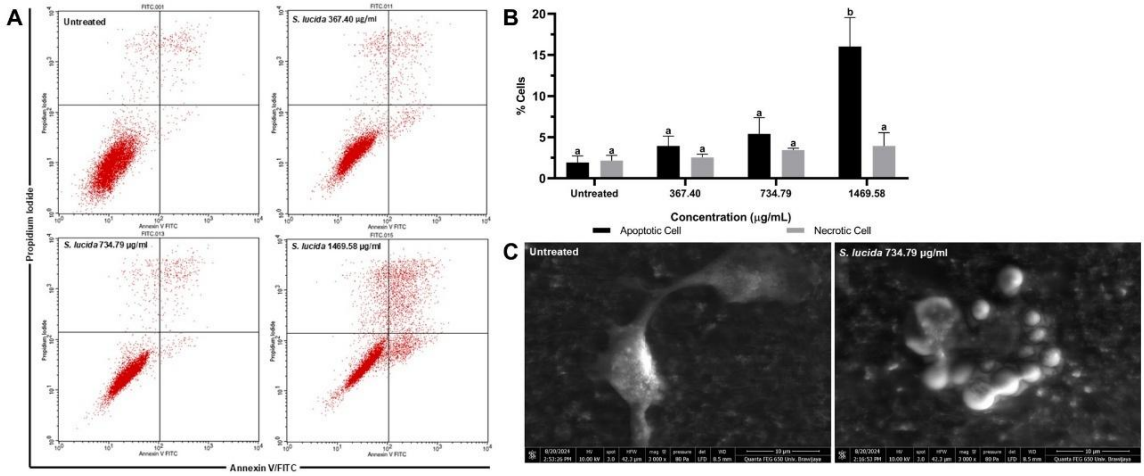

Figure 6 Induction of Apoptosis in T47D Cells by *S. lucida* Stem Extract. (A) - (B) Annexin V/FITC-PI assay demonstrates apoptosis induction in T47D cells following treatment. Bar graphs with different letters denote statistically significant differences between groups ($p \leq 0.05$). Data are presented as mean ± SD. (C) SEM images display the morphological differences between non-apoptotic and apoptotic T47D cells. Cells were cultured directly on carbon tapes for 24 h. Magnification: 3,000×.

SEM is an excellent instrument for examining biological specimens and their ultra-structures, which are not normally visible by light microscopy. To confirm apoptosis in T47D cells by SEM, cells were grown directly on carbon tape, cultured and treated, then fixed, dehydrated and air dried before coating and observation [30]. The observation showed that *S. lucida* stem extract at a concentration of 734.79 µg/mL can induce apoptosis as indicated by the formation of bleb on the surface of a cell (**Figure 6(C)**). Based on the *in silico* results, 6 compounds were found to have anticancer activity related to the apoptotic pathway, namely 3-O-caffeoylquinic acid, adenosine, loganine, secoxyloganin, sweroside and tachioside (**Figure 1**). The compound 3-O-caffeoylquinic acid, or known as chlorogenic acid, is a class of phenolic compounds with pro-oxidative activity, capable of modulating the production of reactive oxygen species (ROS), disrupting the mitochondrial membrane potential, as well as inducing the transcriptional activity of caspase 3, caspase 8, and caspase 9, leading to the activation of the apoptotic pathway [48,49]. These results are in line with the analysis of protein-protein interactions of *S. lucida* targets that interact with the MMP2, MMP9, CASP3, CASP8, and CASP9 protein signaling pathways (**Figure 2**).

Alteration of mitochondrial membrane potential (MPP) in T47D cells by *S. lucida* stem extract

In addition to assessing apoptosis in T47D cells, this study also analyzed changes in mitochondrial membrane potential (MMP). The analysis of MMP in T47D cells with extract administration was evaluated using MitoTracker Red CMXRos and MitoTracker Green FM, which can represent a relative measure of MMP and describe mitochondrial function. MitoTracker Red CMXRos is a red fluorescent dye that stains mitochondria in living cells and its accumulation depends on changes in membrane potential. MitoTracker Green FM is a green fluorescent mitochondrial dye whose activity is related to homeostasis disruption and is independent of MMPs [31,50].

The results showed that *S. lucida* stem extract can affect changes in MMP as measured by MitoTracker Red CMXRos, and the expression intensity of MitoTracker Green FM tended to increase significantly in all extract treatment groups (**Figure 7**). The extract is known to be able to induce a significant decrease in MMP at concentrations of 367.40 and 734.79 µg/mL. The decrease or loss of MMP ($\Delta\psi m$) is closely associated with the activation of cell death pathways or apoptosis markers [51,52].

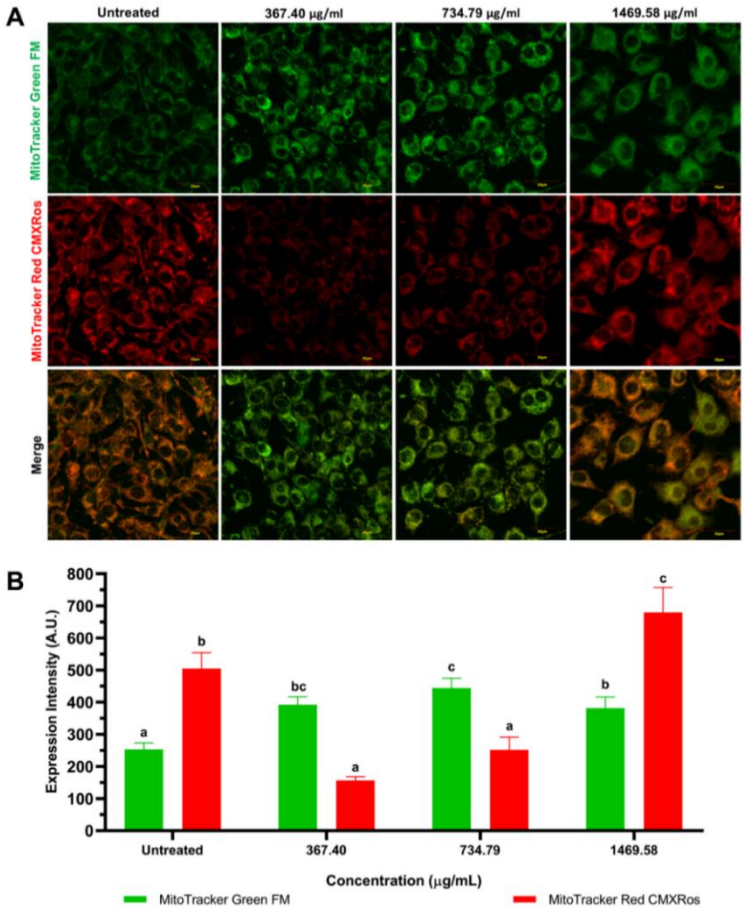

Figure 7 *S. lucida* Stem Extract Triggers Mitochondrial Membrane Potential (MMP) Changes in T47D Cells. (A) CLSM observation of MitoTracker Green FM (green) and MitoTracker Red CMXRos expression in T47D cells. Magnification: 800x. (B) The intensity difference of MitoTracker Green FM and MitoTracker Red CMXRos expression upon administration of *S. lucida* stem extract. Different letters in the graph indicate statistically significant differences between groups ($p \leq 0.05$). Data are presented as mean ± SD.

On the other hand, the results also showed that the extract was able to induce a significant increase in MMPs at the highest concentration (**Figures 7(A) - 7(B)**). During apoptosis, MMPs are not only depolarised following the release of cytochrome c (Cyt c), but the mitochondrial inner membrane can also undergo transient hyperpolarisation during apoptosis. In general, mitochondria in cancer cells are hyperpolarised compared to normal cells. Hyperpolarisation can be caused by increased intracellular Ca^{2+} levels and upregulation of the anti-apoptotic protein BCL-2 in cancer cells. In addition, hyperpolarisation of MMPs in cancer cells can promote the selective transfer of mitochondria-targeting drugs into cancer cells, which can induce cancer cell apoptosis. Mitochondrial membrane hyperpolarisation as an early event associated with mitochondria-dependent apoptosis [53,54]. The increase in MMP by the extract may indicate the early stages of apoptosis in T47D cells.

The use of herbal based products offers significant advantages in addressing the complexities of cancer treatment due to their multi-target mechanisms. In many cases, single-target drug development fails to provide optimal therapeutic outcomes or can lead to resistance, often caused by mutations in the target protein, even during the initial response to treatment. A more holistic, multi-target therapeutic approach that takes into account the multifactorial nature of cancer and the involvement of protein-protein interactions holds great potential for advancing cancer treatment strategies [9,55,56]. *S. lucida* stem ethanol extract has potential as an anticancer herbal candidate that can modulate cancer cell death by several mechanisms, such as pro-oxidative activity of its bioactive compounds, especially phenols, changes in

MMP polarization, and inhibition of the MAPK pathway, which are interrelated and in line with the *in vitro* and *in silico* studies conducted. However, more extensive studies are needed to elucidate the specific mechanism of *S. lucida* stem ethanol extract on the cancer cell death pathway.

Conclusions

This study focuses on *in vitro* and *in silico* approaches to evaluate the anticancer potential of *S. lucida* stem extract on breast cancer cells. Phenolic compounds were the class of compounds with the highest content in *S. lucida* stem extract. There are six *S. lucida* compounds that are predicted to have anticancer activity, namely 3-O-caffeoylquinic acid, adenosine, loganine, secoxyloganin, sweroside and tachioside, which are related to anti-cancer pathways through their interaction with MAPK9 and MAPK3. The extract was moderately toxic to T47D cells and generally cytotoxic to TIG-1 cells. The extract induced apoptosis, while cell morphology analysis revealed the formation of surface blebs, indicating apoptotic cell death. The extract can induce changes in MMP and changes in mitochondrial mass. *S. lucida* stem extract has potential as an anticancer candidate based on the results of *in vitro* and in vivo studies. However, further studies are required to elucidate the mechanism of action of *S. lucida* bioactive compounds in inhibiting breast cancer cells, particularly through mitochondria-related death pathways and MAPK pathway inhibition.

Acknowledgements

This research was funded by Directorate of Research, Technology, and Community Service, The Ministry of Education, Culture, Research, and Technology Republic Indonesia, the National Competition Research - Doctoral Dissertation Research with contract number 1133.2/UN10.C10/TU/2023.

References

[1] E Goodarzi, R Beiranvand, H Naemi, SR Pordanjani and Z Khazaei. Geographical distribution incidence and mortality of breast cancer and its relationship with the human development index (HDI) - an ecology study in 2018. *World Cancer Research Journal* 2020; **7**, e1468.

[2] H Sung, J Ferlay, RL Siegel, M Laversanne, I Soerjomataram, A Jemal and F Bray. Global cancer statistics 2020: GLOBOCAN estimates of incidence and mortality worldwide for 36 cancers in 185 countries. *CA: A Cancer Journal for Clinicians* 2021; **71(3)**, 191-280.

[3] AS Choudhari, PC Mandave, M Deshpande, P Ranjekar and O Prakash. Phytochemicals in cancer treatment: from preclinical studies to clinical practice. *Frontiers in Pharmacology* 2020; **10**.

[4] WF Taylor, SE Moghadam, MM Farimani, SN Ebrahimi, M Tabefam and E Jabbarzadeh. A multi-targeting natural compound with growth inhibitory and anti-angiogenic properties re-sensitizes chemotherapy resistant cancer. *PLoS ONE* 2019; **14(6)**, e0218125.

[5] R Butti, S Das, VP Gunasekaran, AS Yadav, D Kumar and GC Kundu. Receptor tyrosine kinases (RTKs) in breast cancer: signaling, therapeutic implications and challenges. *Molecular Cancer* 2018; **17(1)**, 34.

[6] PA Akinnusi, SO Olubode, AO Adebesin, TA Nana and SA Shodehinde. Discovery of promising inhibitors of epidermal growth factor receptor (EGFR), human epidermal growth factor receptor 2 (HER2), estrogen receptor (ER), and Phosphatidylinositol-3-kinase a (PI3Ka) for personalized breast cancer treatment. *Cancer Inform* 2022; **21**, 1-13.

[7] A Oza and CX Ma. New insights in estrogen receptor (ER) biology and implications for treatment. *Current Breast Cancer Reports* 2017; **9**, 13-25.

[8] TN Aung, Z Qu, RD Kortschak and DL Adelson. Understanding the effectiveness of natural compound mixtures in cancer through their molecular mode of action. *International Journal of Molecular Sciences* 2017; **18(3)**, 656.

[9] M Huang, JJ Lu and J Ding. Natural products in cancer therapy: Past, present and future. *Natural Products and Bioprospecting* 2021; **11**, 5-13.

[10] AAD Rahayu, AI Prihantini, Krisnawati and YMMA Nugraheni. Chemical components of different parts of *Strychnos ligustrina*, a medicinal plant from Indonesia. *IOP Conference Series:*

Earth and Environmental Science 2022; **959**, 012061.

[11] A Setiawansyah, MA Reynaldi, DH Tjahjono and S Sukrasno. Molecular docking-based virtual screening of antidiabetic agents from songga (*Strychnos lucida* R.Br.): An indonesian native plant. *Current Researchon Biosciences and Biotechnology* 2022; **3(2)**, 208-214.

[12] EF Fang, L Froetscher, M Scheibye-Knudsen, VA Bohr, JH Wong and TB Ng. Emerging antitumor activities of the bitter melon (*Momordica charantia*). *Current Protein & Peptide Science* 2019; **20(3)**, 296-301.

[13] L Lu, R Huang, Y Wu, JM Jin, HZ Chen, LJ Zhang and X Luan. Brucine: A review of phytochemistry, pharmacology, and toxicology. *Frontiers in Pharmacology* 2020; **11**, 377.

[14] P Sharma, BP Dwivedee, D Bisht, AK Dash and D Kumar. The chemical constituents and diverse pharmacological importance of *Tinospora cordifolia*. *Heliyon* 2019; **5(9)**, 02437.

[15] S Sur, R Steele, TS Isbell, KN Venkata, ME Rateb and RB Ray. Momordicine-I, a Bitter Melon Bioactive Metabolite, displays Anti-Tumor activity in head and neck cancer involving c-Met and downstream signaling. *Cancers* 2021; **13(6)**, 1432.

[16] N Widodo, S Puspitarini, MH Widyananda, A Alamsyah, ST Wicaksono, M Masruri and YD Jatmiko. Anticancer activity of *Caesalpinia sappan* by downregulating mitochondrial genes in A549 lung cancer cell line. *F1000Research* 2022; **11**, 169.

[17] MH Widyananda, ST Wicaksono, K Rahmawati, S Puspitarini, SM Ulfa, YD Jatmiko, M Masruri and N Widodo. A potential anticancer mechanism of finger root (*Boesenbergia rotunda*) extracts against a breast cancer cell line. *Scientifica* 2022; **2022**, 130252.

[18] A Łukowski, R Jagiełło, P Robakowski, D Adamczyk and P Karolewski. Adaptation of a simple method to determine the total terpenoid content in needles of coniferous trees. *Plant Science* 2022; **314**, 111090.

[19] PV Tan. The determination of total alkaloid, polyphenol, flavonoid and saponin contents of pogang gan (*Curcuma sp.*). *International Journal of Biology* 2018; **10**, 4.

[20] FM Afendi, T Okada, M Yamazaki, A Hirai-Morita, Y Nakamura, K Nakamura, S Ikeda, H Takahashi, Md Altaf-Ul-Amin, LK Darusman, K Saito and S Kanaya. KNApSAcK family databases: integrated metabolite-plant species databases for multifaceted plant research. *Plant and Cell Physiology* 2012; **53(2)**, 1.

[21] DA Filimonov, AA Lagunin, TA Gloriozova, AV Rudik, DS Druzhilovskii, PV Pogodin and VV Poroikov. Prediction of the biological activity spectra of organic compounds using the pass online web resource. *Chemistry of Heterocyclic Compound* 2014; **50(3)**, 444-457.

[22] AP Davis, CJ Grondin, RJ Johnson, D Sciaky, J Wiegers, TC Wiegers and CJ Mattingly. Comparative Toxicogenomics Database (CTD): Update 2021. *Nucleic Acids Research* 2021; **49**, 1138-1143.

[23] SW Marseti, FE Hermanto, MH Widyananda, N Rosyadah, FS Kamila, Y Annisa, DR Dwijayanti, SM Ulfa and N Widodo. Pharmacological potential of *Clinacanthus nutans*: Integrating network pharmacology with experimental studies against lung cancer. *Journal of Biologically Active Products from Nature* 2024; **14(3)**, 343-358.

[24] BT Sherman, M Hao, J Qiu, X Jiao, MW Baseler, HC Lane, T Imamichi and W Chang. DAVID: a web server for functional enrichment analysis and functional annotation of gene lists (2021 update). *Nucleic Acids Research* 2022; **50(1)**, 216-221.

[25] NM O'Boyle, M Banck, CA James, C Morley, T Vandermeersch and GR Hutchison. Open Babel: An open chemical toolbox. *Journal of Cheminformatics* 2011; **3**, 33.

[26] O Trott and AJ Olson. AutoDock Vina: improving the speed and accuracy of docking with a new scoring function, efficient optimization and multithreading. *Journal of Computational Chemistry* 2010; **31(2)**, 455-461.

[27] JM Calderón-Montaño, SM Martínez-Sánchez, V Jiménez-González, E Burgos-Morón, E Guillén-Mancina, JJ Jiménez-Alonso, P Díaz-Ortega, F García, A Aparicio and M López-Lázaro. Screening for selective anticancer activity of 65

extracts of plants collected in western andalusia, spain. *Plants* 2021; **10(10)**, 2193.

[28] JJ Lee, L Saiful Yazan, NK Kassim, CA Che Abdullah, N Esa, PC Lim and DC Tan. Cytotoxic Activity of *Christia vespertilionis* root and leaf extracts and fractions against breast cancer cell lines. *Molecules* 2020; **25(11)**, 2610.

[29] YI Christina, M Rifa'i, N Widodo and MS Djati. Comparative study of antiproliferative activity in different plant parts of *Phaleria macrocarpa* and the underlying mechanism of action. *The Scientific World Journal* 2022; **2022(1)**, 992660.

[30] R Ali, K El-Boubbou and M Boudjelal. An easy, fast and inexpensive method of preparing a biological specimen for scanning electron microscopy (SEM). *MethodsX*. 2021; **8**, 101521.

[31] W Pendergrass, N Wolf and M Poot. Efficacy of MitoTracker Green and CMXrosamine to measure changes in mitochondrial membrane potentials in living cells and tissues. *Cytometry Part A* 2004; **61A(2)**, 162-169.

[32] N da C Sarmento, A Worachartcheewan, R Pingaew, S Prachayasittikul, S Ruchirawat and V Prachayasittikul. Antimicrobial, antioxidant and anticancer activities of *Strychnos lucida* R. *African Journal of Traditional, Complementary and Alternative Medicines* 2015; **12(4)**, 122-127.

[33] X Chen, M Xu and Y An. Identifying the essential nodes in network pharmacology based on multilayer network combined with random walk algorithm. *Journal of Biomedical Informatics* 2021; **114**, 103666.

[34] Y Feng, Q Wang and T Wang. Drug target protein-protein interaction networks: A systematic perspective. *BioMed Research International* 2017; **2017(1)**, 1289259.

[35] A Alexa, O Ember, I Szabó, Y Mo'ath, ÁL Póti, A Reményi and Z Bánóczi. Peptide based inhibitors of protein binding to the Mitogen-Activated protein kinase docking groove. *Frontiers in Molecular Biosciences* 2021; **8**, 690429.

[36] ME Bahar, HJ Kim and DR Kim. Targeting the RAS/RAF/MAPK pathway for cancer therapy: from mechanism to clinical studies. *Signal Transduction and Targeted Therapy* 2023; **8**, 455.

[37] A Kuglstatter, M Ghate, S Tsing, AG Villaseñor, D Shaw, JW Barnett and MF Browner. X-ray crystal structure of JNK2 complexed with the p38α inhibitor BIRB796: Insights into the rational design of DFG-out binding MAP kinase inhibitors. *Bioorganic & Medicinal Chemistry Letters* 2010; **20(17)**, 5217-5220.

[38] T Kinoshita, I Yoshida, S Nakae, K Okita, M Gouda, M Matsubara, K Yokota, H Ishiguro and T Tada. Crystal structure of human mono-phosphorylated ERK1 at Tyr204. *Biochemical and Biophysical Research Communications* 2008; **337(4)**, 1123-1127.

[39] X Liu, CS Zhang, C Lu, SC Lin, JW Wu and ZX Wang. A conserved motif in JNK/p38-specific MAPK phosphatases as a determinant for JNK1 recognition and inactivation. *Nature Communications* 2016; **7**, 10879.

[40] J Shawon, AM Khan, I Shahriar and MA Halim. Improving the binding affinity and interaction of 5-Pentyl-2-Phenoxyphenol against Mycobacterium Enoyl ACP reductase by computational approach. *Informatics in Medicine Unlocked* 2021; **23**, 100528.

[41] A Taherkhani, P Khodadadi, L Samie, Z Azadian and Z Bayat. Flavonoids as strong inhibitors of MAPK3: A computational drug discovery approach. *International Journal of Analytical Chemistry* 2023; **2023(1)**, 8899240.

[42] J Chen, Y Qu, F Li, H Zhang, X Zhang and X Cao. Loganin inhibits liver cancer cell proliferation and metastasis via blocking mitogen-activated protein kinase signaling pathway. *Indian Journal of Pharmaceutical Sciences* 2024; **86(1)**, 163-169.

[43] Y Jeong, SY Bae, D You, SP Jung, HJ Choi, I Kim, SK Lee, J Yu, SW Kim, JE Lee, S Kim and SJ Nam. EGFR is a therapeutic target in hormone Receptor-Positive breast cancer. *Cellular Physiology and Biochemistry* 2019; **53(5)**, 805-819.

[44] R.B. Badisa, S.F. Darling-Reed, P. Joseph, J.S. Cooperwood, L.M. Latinwo, C.B. Goodman, Selective Cytotoxic Activities of Two Novel Synthetic Drugs on Human Breast Carcinoma MCF-7 Cells. *Anticancer Research* 2009; **29**, 2993-2996.

[45] NTT Tram, DH Anh, HH Thuc and NT Tuan. Investigation of chemical constituents and

cytotoxic activity of the lichen Usnea undulata. *Vietnam Journal of Chemistry* 2020; **58(1)**, 63-66.

[46] LC Crowley, BJ Marfell, AP Scott and NJ Waterhouse. Quantitation of apoptosis and necrosis by annexin v binding, propidium iodide uptake, and flow cytometry. *Cold Spring Harbor Protocols* 2016; **11**, 087288.

[47] P Wisitpongpun, N Suphrom, P Potup, N Nuengchamnong, PC Calder and K Usuwanthim. *In vitro* bioassay-guided identification of anticancer properties from *Moringa oleifera* Lam. leaf against the MDA-MB-231 cell line. *Pharmaceuticals* 2020; **13(12)**, 464.

[48] M Kimsa-Dudek, A Synowiec-Wojtarowicz, A Krawczyk, A Kosowska, M Kimsa-Furdzik and T Francuz. The apoptotic effect of caffeic or chlorogenic acid on the C32 cells that have simultaneously been exposed to a static magnetic field. *International Journal of Molecular Sciences* 2022; **23(7)**, 3859.

[49] JS Yang, CW Liu, YS Ma, SW Weng, NY Tang, SH Wu, BC Ji, CY Ma, YC Ko, S Funayama and CL Kuo. Chlorogenic acid induces apoptotic cell death in U937 leukemia cells through caspase- and Mitochondria-dependent pathways. *In Vivo* 2012; **26**, 971-978.

[50] K Neikirk, AG Marshall, B Kula, N Smith, S LeBlanc and A Hinton. MitoTracker: A useful tool in need of better alternatives. *European Journal of Cell Biology* 2023; **102(4)**, 151371.

[51] S Kari, K Subramanian, IA Altomonte, A Murugesan, O Yli-Harja and M Kandhavelu. Programmed cell death detection methods: A systematic review and a categorical comparison. *Apoptosis* 2022; **27**, 482-508.

[52] MH Widyananda, L Muflikhah, SM Ulfa and N Widodo. Unveiling the antibreast cancer mechanism of *Euphorbia hirta* ethanol extract: Computational and experimental study. *Journal of Biologically Active Products from Nature* 2024; **14(3)**, 359-382.

[53] S Mani, G Swargiary and KK Singh. Natural agents targeting mitochondria in cancer. *International Journal of Molecular Sciences* 2020; **21(19)**, 6992.

[54] S Matsuyama and JC Reed. Mitochondria-dependent apoptosis and cellular pH regulation. *Cell Death and Differentiation* 2000; **7**, 1155-1165.

[55] J Mann. Natural products in cancer chemotherapy: Past, present and future. *Nature Reviews Cancer* 2002; **2**, 143-148.

[56] MH Widyananda, SK Pratama, RS Samoedra, FN Sari, VD Kharisma, ANM Ansori and Y Antonius. Molecular docking study of sea urchin (*Arbacia lixula*) peptides as multi-target inhibitor for non-small cell lung cancer (NSCLC) associated proteins. *Journal of Pharmacy & Pharmacognosy Research* 2021; **9(4)**, 484-496.